Two-dimensional lattice vesicles and polygons

1991 J. Phys. A: Math. Gen. 24 3095

(http://iopscience.iop.org/0305-4470/24/13/023)

J. Phys. A: Math. Gen. 24 (1991) 3095-3106. Printed in the UK

Two-dimensional lattice vesicles and polygons

Michael E Fisher†, Anthony J Guttmann‡ and Stuart G Whittington§

† Institute for Physical Science and Technology, University of Maryland, College Park, MD 20742, USA

‡ Department of Mathematics, The University of Melbourne, Parkville, Victoria 3052, Australia

§ Department of Chemistry, University of Toronto, Toronto, Canada M5S 1A1

Received 13 December 1990, in final form 26 March 1991

Abstract. We consider a lattice model of two-dimensional vesicles, in which the boundary of the vesicle is the perimeter of a self-avoiding polygon embeddable in the square lattice. With fixed boundary length m we incorporate an osmotic pressure difference by associating a fugacity with the area enclosed by the polygon. We derive rigorous results concerning the behaviour of the associated free energy and the form of the phase diagram. By deriving exact values of the numbers of polygons with m edges which enclose area n, and analysing the resulting series, we obtain the free energy, the phase boundary and various scaling exponents and amplitudes numerically.

1. Introduction and summary

Biological membranes consist of lipid bilayers and, when closed, form vesicles. These vesicles form a variety of shapes, depending on the pH, osmotic pressure, temperature, etc. In an attempt to understand the shapes which can be assumed under the influence of thermal fluctuations, the corresponding problem in two dimensions has recently been studied by Leibler, Singh and Fisher [1, 2] through Monte Carlo simulations and scaling arguments. A convenient model for the boundary of the two-dimensional vesicle is a polygon either in the continuum or on a lattice. The polygon is taken to be self-avoiding and one asks, in the lattice version, for the number of polygons with m edges enclosing area n [1-3]. One can also ask for the dimensions of the polygon, at fixed number of edges in the perimeter, as a function of a fugacity associated with the enclosed area [1, 2]. These problems clearly have interest in their own rights independent of their potential biological implications.

For the pure polygon problem (i.e. at unit fugacity) the mean-square radius of gyration scales as $m^{2\nu}$, where ν is the self-avoiding walk size exponent [1]. The area is expected to scale in the same way [1] and Enting and Guttmann [3] have recently confirmed this feature in the lattice model using exact enumeration and series analysis methods. Conversely, one can ask how the perimeter scales with the area. Enting and Guttmann [3] used series analysis techniques to show that the perimeter scales with the first power of the area and Janse van Rensburg and Whittington [4] subsequently proved this result rigorously.

In this paper we consider the number $v_m(n)$ of polygons per site on an indefinitely large square lattice with m edges enclosing area n. We show rigorously that the

0305-4470/91/133095+12$03.50

free-energy-like limit

$$\lim_{m\to\infty} m^{-1} \log \sum_{n} v_m(n) y^n \equiv \tilde{\kappa}(y) \tag{1.1}$$

exists and is finite for all values of the fugacity $y \leq 1$, and, furthermore, that $\tilde{\kappa}(y)$ is log-convex and continuous for these values of y. However, we prove that the limit is infinite for $y > 1$.

It is also natural to define the two-variable generating function or 'grand partition function'

$$P(x, y) = \sum_{x,y} v_m(n) x^m y^n. \tag{1.2}$$

We show that, for $y < 1$, $P(x, y)$ converges for $x < e^{-\tilde{\kappa}(y)}$. For $y > 1$, $P(x, y)$ converges only for $x = 0$. These results can be expressed in terms of a phase diagram in the space of the two fugacities x and y. The form of this phase diagram is shown in figure 1. For $x < e^{-\tilde{\kappa}(y)}$ and $y < 1$ the polygons are ramified objects, closely resembling branched polymers. (In fact the corresponding graphs on the dual lattice are a subset of site animals.) As y approaches unity less ramified configurations predominate; at $y = 1$ one has standard self-avoiding polygons. This region, $\{x < e^{-\tilde{\kappa}(y)}, y \leq 1\}$ might be referred to as the 'droplet' or 'compact' phase. For $y > 1$ the polygons become 'expanded' or 'inflated' and approximate squares, their average areas scaling as the square of their perimeters. In this article we do not directly address the behaviour for $y < 1$ *above* the phase boundary (i.e. for $x > e^{-\tilde{\kappa}(y)}$). We expect, however, that (on considering the thermodynamic limit of a sequence of finite lattices) this phase can be described as a single convoluted polygon that 'fills' the whole lattice rather like a closed Hamiltonian walk: one might describe it as a 'seaweed phase'.

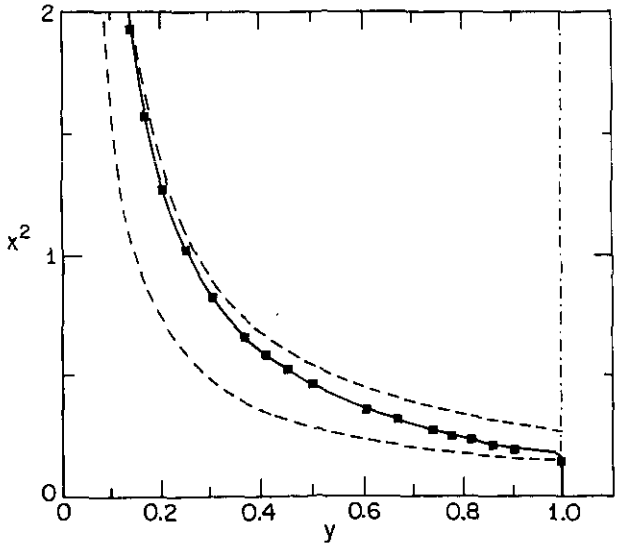

Figure 1. Plot of the phase boundary $y_c(x)$ or, equivalently, $x_c(y)$: solid squares; the curve is merely a guide to the eye. The series expansions for the generating function $P(x, y)$ converge on the origin side of the phase boundary and on the vertical piece at $y = 1$: this region defines the *droplet* or *compact* phase. For $y > 1$ the polygons are highly *expanded*; for $y < 1$ but above the boundary, a seaweed-like phase is anticipated. The broken curves denote upper and lower bounds for the phase boundary: see text for details.

In section 3 we obtain the form of the phase diagram numerically from analysis of appropriate series and analyse the behaviour in the region of the multicritical point at $(x = e^{-\tilde{\kappa}(1)}, y = 1)$ using scaling concepts.

2. Some rigorous results

Let $v_m(n)$ be the number of polygons, per lattice site, weakly embeddable in the two-dimensional square lattice, with m edges enclosing area n. Let

$$p_m = \sum_n v_m(n) \tag{2.1}$$

and let

$$a_n = \sum_m v_m(n) \tag{2.2}$$

so that p_m is the number of polygons with m edges and a_n is the number of polygons with area n. For example, $p_4 = 1$, $p_6 = 2$, $a_1 = 1$ and $a_2 = 2$. We define the generating functions

$$P_m(y) = \sum_n v_m(n) y^n \tag{2.3}$$

$$A_n(x) = \sum_m v_m(n) x^m \tag{2.4}$$

and

$$P(x, y) = \sum_{m,n} v_m(n) x^m y^n = \sum_m P_m(y) x^m = \sum_n A_n(x) y^n. \tag{2.5}$$

Consider first polygons with maximum area for fixed perimeter. If the perimeter m is a multiple of 4, the maximum area is clearly $m^2/16$, while if 4 does not divide m the maximum area is $(m^2 - 4)/16$. We focus initially on the case $y > 1$. Since $P_m(y)$ is not less than any term in (2.3), taking n to be the maximum area yields

$$\liminf_{m \to \infty} m^{-2} \log P_m(y) \geqslant \frac{\log y}{16}. \tag{2.6}$$

Similarly

$$P_m(y) \leqslant p_m y^{m^2/16} \tag{2.7}$$

and, since [5]

$$p_m = e^{\kappa m + o(m)} \tag{2.8}$$

where κ is the connective constant of the lattice (or the self-avoiding walk limit), we have

$$\lim_{m \to \infty} m^{-2} \log P_m(y) = \frac{\log y}{16} \tag{2.9}$$

for all $y \geqslant 1$.

This result has interesting implications for the behaviour of the average area

$$\bar{n}_m(y) \equiv \langle n(m) \rangle = \sum_n n v_m(n) y^n / \sum_n v_m(n) y^n \tag{2.10}$$

when $y > 1$. To see this, note first that $L_m(\log y) \equiv \log P_m(y)$ is a convex function of $\log y$ for all m. This is proved easily with the aid of Cauchy's inequality which gives

$$\begin{aligned} P_m(y_1)P_m(y_2) &= \sum_{n_1} v_m(n_1) y_1^{n_1} \sum_{n_2} v_m(n_2) y_2^{n_2} \\ &\geqslant \left(\sum_n v_m(n)(y_1 y_2)^{n/2} \right)^2 \\ &= [P_m(\sqrt{y_1 y_2})]^2. \end{aligned} \tag{2.11}$$

It remains only to take logarithms. It follows from this that the area functions

$$k_m(y) \equiv \bar{n}_m(y)/m^2 = m^{-2} \partial L_m(\log y)/\partial \log y \tag{2.12}$$

are the derivatives of a sequence of convex functions $l_m(\log y) = m^{-2} L_m(\log y)$ which, by (2.9), approach a limit. Furthermore, the limit is also differentiable with

$$k_\infty(y) = \partial l_\infty(\log y)/\partial \log y = \tfrac{1}{16}. \tag{2.13}$$

In the circumstances a lemma on sequences of convex functions [6] implies that $k_m(y) \to k_\infty(y)$ and hence we conclude that

$$\lim_{m \to \infty} \bar{n}_m(y)/m^2 = \tfrac{1}{16}. \tag{2.14}$$

This is independent of y and the qualitative change in behaviour occurs as soon as y is greater than unity. (There is no effective entropic restoring force since this scales with m, not with m^2.)

For the case $y \leqslant 1$ we note that $P_m(y) \leqslant p_m$ so, from (2.8), $\limsup_{m \to \infty} m^{-1} \log P_m(y)$ is bounded above by κ. By a standard concatenation construction in which two vesicles are joined by a 'neck' consisting of a single square, we obtain a larger vesicle and thereby find

$$v_{m_1+m_2}(n) \geqslant \sum_{n_1} v_{m_1}(n_1) v_{m_2}(n - n_1 - 1). \tag{2.15}$$

Multiplying (2.15) by y^n and summing over n gives

$$y P_{m_1+m_2}(y) \geqslant [y P_{m_1}(y)][y P_{m_2}(y)]. \tag{2.16}$$

Since $m^{-1} \log[y P_m(y)]$ is bounded above for $y \leqslant 1$, this implies that

$$\tilde{\kappa}(y) \equiv \lim_{m \to \infty} m^{-1} \log P_m(y) \tag{2.17}$$

exists and is finite for $0 < y \leqslant 1$ [7]. Moreover, if we define

$$f_m(y) = [y P_m(y)]^{1/m} \tag{2.18}$$

then (2.15) implies that [7]

$$\sup_{m>0} f_m(y) = \lim_{m \to \infty} f_m(y) \equiv f(y) = \mathrm{e}^{\tilde{\kappa}(y)}. \tag{2.19}$$

Note that $\tilde{\kappa}(1) = \kappa$, is the connective constant.

Since $P_m(y)$ is monotone increasing in y, the limit $\tilde{\kappa}(y)$ is monotone non-decreasing and therefore to prove that $\tilde{\kappa}(y)$ is log-convex it suffices to show that

$$\frac{\tilde{\kappa}(y_1) + \tilde{\kappa}(y_2)}{2} \geqslant \tilde{\kappa}(\sqrt{y_1 y_2}). \tag{2.20}$$

This follows immediately from (2.11); it is only necessary to take logarithms, divide by m and let $m \to \infty$. The convexity establishes that $\tilde{\kappa}(y)$ is continuous in the interval $[0, 1)$.

To prove left-continuity at $y = 1$ we argue as follows. For each $\varepsilon > 0$ we can choose m sufficiently large that

$$f(1) - f_m(1) < \varepsilon/2. \tag{2.21}$$

With this value of m fixed there exists $\delta > 0$ such that

$$f_m(1) - f_m(1-\delta) < \varepsilon/2 \tag{2.22}$$

since $f_m(y)$ is continuous. But (2.19) implies that $f_m(1-\delta) \leqslant f(1-\delta)$ which, together with (2.21) and (2.22), gives

$$f(1) - f(1-\delta) < \varepsilon \tag{2.23}$$

so that $f(y)$, and hence $\tilde{\kappa}(y)$ is left-continuous at $y = 1$.

Now for fixed perimeter m the minimum area is

$$n_{\min}(m) = (m-2)/2 \tag{2.24}$$

so that for $y \leqslant 1$ we have

$$P_m(y) \leqslant p_m y^{(m-2)/2} \tag{2.25}$$

and thus obtain the bound

$$\tilde{\kappa}(y) \leqslant \kappa + \tfrac{1}{2} \log y. \tag{2.26}$$

Similarly, by picking out a particular term in the series in (2.3), we have

$$P_m(y) \geqslant v_m[(m-2)/2] y^{(m-2)/2}. \tag{2.27}$$

The number of polygons with perimeter m and minimum area is just the number of a certain class of site trees on the dual lattice having $(m-2)/2$ vertices. These can be concatenated to prove the existence of a thermodynamic limit which we denote as κ_0. Thence we find the lower bound

$$\tilde{\kappa}(y) \geqslant \tfrac{1}{2}\kappa_0 + \tfrac{1}{2} \log y. \tag{2.28}$$

These upper and lower bounds for $\tilde{\kappa}(y)$ together imply

$$\lim_{y \to 0+} \tilde{\kappa}(y)/\log y = \tfrac{1}{2}. \tag{2.29}$$

The generating function $P(x, y)$ can be written using (2.17) as

$$P(x, y) = \sum_m P_m(y) x^m = \sum_m \mathrm{e}^{m\tilde{\kappa}(y) + o(m)} x^m \tag{2.30}$$

and for fixed x this converges for $x < \mathrm{e}^{-\tilde{\kappa}(y)}$ so that the phase boundary is given by the curve

$$x = x_c(y) \equiv \mathrm{e}^{-\tilde{\kappa}(y)}. \tag{2.31}$$

The behaviour of $\tilde{\kappa}(y)$ as $\log y \to -\infty$ is given by (2.29) and this implies that x_c goes to infinity as

$$x_c(y) \sim y^{-1/2} \tag{2.32}$$

when $y \to 0$.

Since $\tilde{\kappa}(y)$ is monotone non-decreasing, $x_c(y)$ is monotone non-increasing. In addition x_c is bounded below by $e^{-\kappa}$ for $y \leqslant 1$ and then jumps discontinuously to zero: see figure 1. The two bounds (2.26) and (2.28) imply that the phase boundary satisfies

$$e^{-\kappa_0} \geqslant x_c^2 y \geqslant e^{-2\kappa}. \tag{2.33}$$

In a similar way we can derive asymptotic results for the generating function $A_n(x)$. Setting $x = 1$ we have $A_n(1) = a_n$ and a concatenation construction as used in (2.15) immediately gives

$$a_n = e^{\chi n + o(n)}. \tag{2.34}$$

For $x \leqslant 1$, one has $A_n(x) \leqslant a_n$ while for $x > 1$ one obtains

$$A_n(x) \leqslant a_n x^{m_{\max}} = a_n x^{2(n+1)} \tag{2.35}$$

so that $n^{-1} \log A_n(x)$ is bounded above for all $x < \infty$. Then the concatenation argument establishes the existence of the limit

$$\lim_{n\to\infty} n^{-1} \log A_n(x) = \tilde{\chi}(x) \tag{2.36}$$

and, similarly, it is easy to show that $\tilde{\chi}(x)$ is log-convex. Since $A_n(x)$ is monotone it follows that $\tilde{\chi}(x)$ is monotone and so $\tilde{\chi}(x) \geqslant \tilde{\chi}(1)$ for $x \geqslant 1$. Similarly, for $x \geqslant 1$, we obtain

$$a_n x^{2n+2} \geqslant A_n(x) \geqslant v_{2n+2}(n) x^{2n+2} \tag{2.37}$$

and hence

$$\chi + 2 \log x \geqslant \tilde{\chi}(x) \geqslant \lim_{n\to\infty} n^{-1} \log v_{2n+2}(n) + 2 \log x. \tag{2.38}$$

It follows immediately that

$$\lim_{x\to\infty} \frac{\tilde{\chi}(x)}{\log x} = 2. \tag{2.39}$$

For $x \leqslant 1$ we have, using an inequality from [5],

$$A_n(x) = \sum_m v_m(n) x^m \leqslant \sum_m p_m x^m \leqslant \sum_{k=2}^{n+1} (e^{\kappa} x)^{2k} \tag{2.40}$$

so that

$$\tilde{\chi}(x) \leqslant 2\kappa + 2 \log x \tag{2.41}$$

when $e^{-\kappa} \leqslant x \leqslant 1$, and $\tilde{\chi}(x) = 0$ when $x \leqslant e^{-\kappa}$. Note that we expect $y_c(x) \equiv e^{-\tilde{\chi}(x)}$ to be the inverse function of $x_c(y)$ discussed above although we have not proved this.

By (2.5) the $A_n(x)$ are the expansion coefficients for $P(x, y)$ in powers of y at fixed x. Our arguments prove that for $x < x_c(1) = e^{-\kappa}$ the radius of convergence of this series is $y_c(x) = 1$. Evidently, then, $P(x, y)$ exhibits a line of nonanalyticities as $y \to 1-$ for $x < e^{-\kappa}$. On the other hand, an easy extension of the arguments shows that *all* the derivatives $(\partial^k P/\partial y^k)$ remain bounded as $y \to 1-$ for $x < e^{-\kappa}$. It follows that the line $y = 1$ for $0 < x < x_c(1)$ is a line of essential singularities. This conclusion (and, indeed, the argument) is the same as that concerning the existence of 'droplet singularities' at a point of condensation or first-order phase transition as developed some time ago by Fisher [8] (see also Andreev [9] and Isakov [10]).

Similar arguments work in three and, indeed, in $d>3$ dimensions. In the three-dimensional case we consider surfaces in Z^3 made up of elementary unit squares, or plaquettes [11]. Let $s_m(n)$ be the number of surfaces per lattice site, homeomorphic to a sphere, having area m and enclosing volume n. We write

$$\mathscr{A}_m(y)=\sum_n s_m(n)y^n \tag{2.42}$$

so that $\mathscr{A}_m(1)\equiv\mathscr{A}_m$ is the number of surfaces with area m.

For the case $y\geqslant 1$ let us focus on surfaces with maximum volume for given surface area. Then it is easy to prove that

$$\lim_{m\to\infty} m^{-3/2}\log \mathscr{A}_m(y)=6^{-3/2}\log y. \tag{2.43}$$

We note that the value of this limit goes to zero as $y\to 1+$.

The surfaces can be concatenated in pairs [11] as in (2.15) to yield the inequality

$$s_{m_1+m_2+2}(n)\geqslant\sum_{n_1} s_{m_1}(n_1)s_{m_2}(n-n_1-1). \tag{2.44}$$

Moreover, $\mathscr{A}_m$ is exponentially bounded above [12] so that, since $\mathscr{A}_m(y)\leqslant\mathscr{A}_m$ for $y\leqslant 1$, it is straightforward to prove the existence of the limit

$$0<\tilde{\Theta}(y)=\lim_{m\to\infty} m^{-1}\log \mathscr{A}_m(y)<\infty \tag{2.45}$$

for all $y\leqslant 1$, and to show that $\tilde{\Theta}(y)$ is log-convex and hence continuous in $[0,1)$. Left-continuity at $y=1$ follows from a minor extension of the argument given for the two-dimensional case. At fixed area m the minimum volume is given by

$$n_{\min}(m)=(m-2)/4. \tag{2.46}$$

For $y\leqslant 1$ we thus have

$$s_m(n_{\min})y^{n_{\min}}\leqslant\mathscr{A}_m(y)\leqslant\mathscr{A}_m y^{n_{\min}} \tag{2.47}$$

so that

$$\Theta_0+\tfrac{1}{4}\log y\leqslant\tilde{\Theta}(y)\leqslant\Theta+\tfrac{1}{4}\log y \tag{2.48}$$

where $\Theta=\tilde{\Theta}(1)$ and

$$\Theta_0=\lim_{m\to\infty} m^{-1}\log \mathscr{A}_m(n_{\min}). \tag{2.49}$$

If we write

$$\mathscr{P}(x,y)=\sum_{m,n} s_m(n)x^m y^n=\sum_m \mathscr{A}_m(y)x^m=\sum_m \mathrm{e}^{m\tilde{\Theta}(y)+o(m)}x^m \tag{2.50}$$

we see that the phase boundary is given by $x_c=\mathrm{e}^{-\tilde{\Theta}(y)}$ and, as $y\to 0$,

$$x_c(y)\sim y^{-1/4}. \tag{2.51}$$

As in two dimensions, the phase boundary $x_c(y)$ is monotone non-increasing and jumps discontinuously to zero at $y=1$. More generally the exponent in this last result is just $1/2^{(d-1)}$. Again essential singularities arise at $y=1$ for $x<x_c(1)$ [8].

3. The phase diagram in two dimensions

From the series given to order $m = 42$ in Enting and Guttmann [3], together with data for $m = 44$ (Guttmann, to be published), we have formed the series $A_n(x)$ at fixed values of x in the range $[e^{-\kappa}, e]$. These we have analysed by the method of differential approximants [13] at each value of x, in order to find the corresponding critical point $y_c(x)$. At $y = 1$, corresponding to $x = e^{-\kappa} \simeq 0.379\,052$ we recover the ordinary perimeter generating function for polygons, which is singular at $y = y_c(e^{-\kappa}) = 1$. For $x > e^{-\kappa}$, $y_c(x)$ montonically decreases as x increases. The estimated values are shown in table 1. Along this line, the critical exponent for $A_n(x)$ is found to be zero, corresponding to a logarithmic divergence of $P(x, y)$ as $y \to y_c(x)$ (or possibly some more complicated logarithmic function yielding a zero exponent). This is just the branched polymer critical exponent [14], as expected along the critical line [1, 2]. In fact the differential approximant analysis only clearly reveals this value of the exponent for $x > 0.6$. For $x < 0.6$ crossover effects manifest themselves for, at the self-avoiding walk limit $y = 1$, the exponent is expected to change discontinuously to $2 - \alpha_0 = 1.5$, the pure self-avoiding polygon exponent [15]. For $x < 0.6$, it is increasingly difficult to estimate $y_c(x)$ for this reason. The exponent given by the differential approximants steadily increases from 0 to 1.5 (its correct value) at $y = 1$, as x decreases from about 0.6 to $e^{-\kappa}$. While we have not quoted confidence limits, we expect errors only in the last quoted digit of $y_c(x)$.

At $y = 1$ there is a vertical condensation line from $(1, 0)$ to $(1, e^{-\kappa})$. The complete phase boundary as established in this way is shown in figure 1. As $y \to 1-$, the phase boundary approaches $(1, e^{-\kappa})$ continuously. From the results of the previous section, we can also derive upper and lower bounds on the phase boundary. However, these bounds require knowledge of two critical points if numerical values are to be obtained. The lower bound is given by $x_c > e^{-\kappa} y^{-1/2}$ and the upper bound by $x_c \leqslant (e^{\kappa_0} y)^{-1/2}$, where $e^{\kappa} \simeq 2.638\,1585$ is the usual square lattice self-avoiding walk connective constant and $e^{\kappa_0} \simeq 1.9269$ is the analogous quantity for those polygons with minimum area for a given perimeter. The lower bound becomes exact as $y \to 1-$, while the upper bound becomes exact as $y \to 0+$. We also show these bounds in figure 1. The upper bound is given by the critical point of the series whose coefficients are polygons with minimum area. This series is given in table 2.

Table 1. Points on the phase boundary determined by differential approximants. Note that $P(x, y)$ diverges logarithmically along this phase boundary: see (3.4).

x	$y_c(x)$	x	$y_c(x)$
2.7183	0.03615	0.9048	0.3020
2.4596	0.04406	0.8187	0.360
2.2255	0.05372	0.7408	0.430
2.0137	0.06540	0.6703	0.505
1.8221	0.07961	0.6065	0.595
1.6487	0.09679	0.5488	0.69
1.4918	0.11758	0.4966	0.79
1.3499	0.14266	0.4493	0.88
1.2214	0.1728	0.4066	0.95
1.1052	0.2089	0.37905	1.000
1.0000	0.25183		

Table 2. Series used in the analysis to determine the crossover exponent, bounds on the phase boundary and the slope of the scaling axes. Due to a typographical error, the coefficient for $m = 42$ was given incorrectly in [3]. The coefficient for $m = 44$ has not been given previously.

m	$p_m(n_{min})$	$y\partial \log P(x, y)/\partial y\|_{y=1}$	$\partial P(x, y)/\partial y\|_{y=1}$
0	0	1	0
2	0	2	0
4	1	11	1
6	2	60	4
8	6	349	22
10	18	2 090	124
12	55	12 833	726
14	174	80 084	4 352
16	566	505 917	26 614
18	1 868	3 226 854	165 204
20	6 237	20 742 407	1 037 672
22	21 050	134 194 920	6 580 424
24	71 666	872 912 333	42 062 040
26	245 696	5704 551 866	270 661 328
28	847 317		1 751 614 248
30	2 937 116		11 391 756 176
32	10 226 574		
34	35 746 292		
36	125 380 257		
38	441 125 966		
40	1 556 301 578		
42	5 504 340 656		
44	19 511 769 838		

The information contained in the phase digram is equivalent to the dependence of the free energy on the area fugacity, as discussed in section 2. There we also discussed the dependence of the appropriate free energy on perimeter fugacity x. We show the numerical estimates of this behaviour, and the upper and lower bounds, in figure 2. The results in this figure are equivalent to the phase diagram given in figure 1 (as mentioned above), in that if the phase boundary is approached at constant y the grand partition function, $P(x, y)$, converges for $y < e^{-\tilde{x}(x)}$.

We now turn to the scaling form of the generating function in the vicinity of the multicritical point $x = x_c$, $y = 1$. We denote deviations from this point by $\Delta x = x_c - x$, $\Delta y = 1 - y$ with Δx, $\Delta y \geqslant 0$. We assume that $y = 1$ is a scaling axis† so that the linear scaling fields are

$$\tilde{x} = \Delta x - \Delta y / e_2 \tag{3.1}$$

where e_2 determines the slope of the second scaling axis, and

$$\tilde{y} = \Delta y. \tag{3.2}$$

Then, ignoring confluent corrections to scaling, we expect the multicritical behaviour in the vicinity of the multicritical point to be described by

$$P(x, y) \approx C_0 |\tilde{x}|^{2-\alpha_0} Z(\tilde{y}/|\tilde{x}|^{\phi}) + B(x, y) \tag{3.3}$$

† As is usual in the theory of bicritical points, we expect a scaling axis parallel to the condensation line, with slope given by dx_c/dy, which in this case gives vertical slope. Figure 1, of course, supports this.

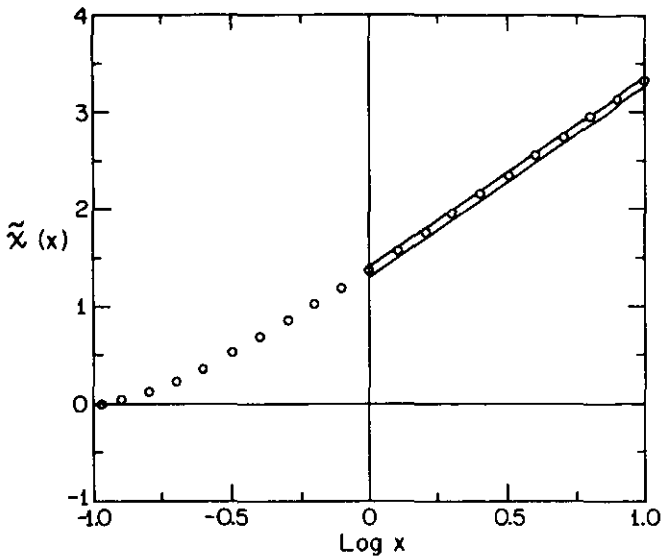

Figure 2. Plot of the reduced free energy, $\tilde{\chi}(x)$, for polygons of perimeter weighted by fugacity x. The two ruled lines for $\log x \geqslant 0$ ($x \geqslant 1$) represent the bounds of (2.38).

where $\alpha_0 = \frac{1}{2}$ is the usual polygon exponent [16], $Z(z)$ is a scaling function with normalization $Z(0) = 1$, ϕ is the crossover exponent and we expect $\phi = 2\nu$ where $\nu = \frac{3}{4}$ is the usual self-avoiding walk correlation function exponent [15], since y is the variable conjugate to the area n which should scale like the mean square size [1, 2]. The term $B(x, y)$ is the analytic background term around (x_c, y_c). At (x_c, y_c) the expected polygon-like critical behaviour is given by the term $C_0|\tilde{x}|^{2-\alpha_0}$, while along the critical isotherm for $y < 1$ the behaviour is expected to be

$$P(x, y) \approx D_0(y) + D_1(y)|\hat{x}|^{2-\hat{\alpha}} \tag{3.4}$$

where $\hat{x}$ measures the distance from the critical line, and $\hat{\alpha}$ is the specific heat exponent corresponding to collapsed polygons, which is expected to be in the same universality class as branched polymers [1, 2, 14] as noted above; in this case we have $\hat{\alpha} = 2$ so that a factor $\log|\hat{x}|$ (possibly to a non-trivial power) should appear in place of $|\hat{x}|^{2-\hat{\alpha}}$.

To estimate the crossover exponent ϕ, we construct the series expansion of

$$y\partial \log P(x, y)/\partial y|_{y=1}$$
$$\equiv N(x, 1) = \sum_n np_m(n)x^m y^n / \sum_n p_m(n)x^m y^n \sim |\tilde{x}|^{2-\alpha_0-\phi}. \tag{3.5}$$

At first sight it might be thought that the behaviour should be $|\tilde{x}|^{-\phi}$, but the denominator is dominated by the analytic term $B(x, y)$, rather than the singular term, with the result that the expected behaviour is as shown. We have constructed the series expansion of $A(x, 1)$, and analysed it by the method of differential approximants. As expected, it is found to be singular at $x = x_c$, and the exponent is found to be -0.04 ± 0.04. As $\alpha = \frac{1}{2}$ this gives $\phi = 1.54 \pm 0.04$, which is entirely consistent with the expected behaviour $\phi = 2\nu = \frac{3}{2}$. This result can also be anticipated from [3], in which it was shown that the mean area of polygons with perimeter n behaves asymptotically as $n^{1.5}$; see also Camacho and Fisher [17]. Alternatively, the series expansion of

$$y\partial P(x, y)/\partial y|_{y=1} = \sum np_m(n)x^m y^n \sim |\tilde{x}|^{2-\alpha_0-\phi} \tag{3.6}$$

can be used to estimate ϕ. This series is also given in table 2, and an analysis similar to that described above gives $\phi = 1.498 \pm 0.002$.

We next turn to the question of the slope of the scaling axis e_2. We estimate this using a method developed by Singh and Fisher [18]. From (3.3) we find

$$\partial P/\partial y|_{y=1} \approx -C_0 Z'(0)|\tilde{x}|^{2-\alpha_0-\phi} + (2-\alpha_0) C_0 |\tilde{x}|^{1-\alpha_0}/e_2 \tag{3.7}$$

while

$$x\partial P/\partial x|_{y=1} \approx -(2-\alpha_0) C_0 x_c |\tilde{x}|^{1-\alpha_0} \tag{3.8}$$

so that a variable multiple of the second term, added to the first, can cancel the confluent term with exponent $1-\alpha_0$. The procedure used in [18] and followed here was to construct the two series, and then to vary the multiple until the best estimate of the (accurately known) critical point and (exactly known) critical exponent is obtained. The first series is given in table 2, the second series follows from the polygon generating function [16]. The appropriate multiple was found to be 0.025 ± 0.025 which translates to a scaling axis slope of $1/e_2 = -0.01 \pm 0.01$. That is, we cannot rule out a horizontal scaling axis.

We have also refined the estimate of the amplitude of the mean area series

$$\tilde{n}_m(1) = \sum n v_m(n) / \sum v_m(n) = N_0 m^{2\nu}[1 + o(1)] \tag{3.9}$$

which is related to the first term Z_1 in the expansion of the scaling function

$$Z(z) = 1 + Z_1 z + O(z^2). \tag{3.10}$$

Using the data in [3] we find, with the aid of a Neville table analysis, $N_0 = 0.1416 \pm 0.0001$. A reanalysis of the data of Privman and Rudnick [19] for the radius of gyration of self-avoiding polygons

$$\langle R_G^2 \rangle \approx M_0 n^{2\nu} \tag{3.11}$$

leads to an estimate for the amplitude of $M_0 = 0.0564 \pm 0.0001$. The ratio is $N_0/M_0 = 2.511 \pm 0.006$. This is less than π as expected, and refines the estimate 2.52 ± 0.04 of this universal ratio found by Camacho and Fisher [17].

Finally we note that the behaviour of the critical line $x_c(y)$ near $y_c = 1$ can be found from the scaling form (3.3) by observing that the scaling function $Z(z)$ will exhibit singular behaviour at some point, say z_c. If $z_c < \infty$, as seems probable from the numerical estimates for $x_c(y)$, the critical line is determined by $\tilde{y}/|\tilde{x}_c|^{\phi} = z_c$ which yields

$$x_c(y) \approx x_c(1) + (\Delta y/z_c)^{2/3} + \Delta y/e_2 + \ldots . \tag{3.12}$$

As mentioned in section 2, the derivative dx_c/dy is expected to diverge as $y \to 1-$. Partial differential approximants [20, 21] provide a systematic route to the estimation of z_c and of $x_c(y)$ near $y_c = 1$ where, as mentioned, strong crossover effects hamper single-variable methods.

Acknowledgments

MEF acknowledges some support from the National Science Foundation (currently under Grant No. DMR 90-07811); AJG was supported by the Australian Research

Council and SGW by NSERC of Canada. SGW would like to acknowledge helpful conversations with Neal Madras and with John Wilker. Some of this work was carried out while SGW was visiting the Mathematics Department at the University of Melbourne and he is grateful to the members of that department for their hospitality.

References

[1] Leibler S, Singh R R P and Fisher M E 1987 *Phys. Rev. Lett.* **59** 1989
[2] Fisher M E 1989 *Physica* D **38** 112
[3] Enting I G and Guttmann A J 1990 *J. Stat. Phys.* **58** 475
[4] Janse van Rensburg E J and Whittington S G 1990 *J. Phys. A: Math. Gen.* **23** 1287
[5] Hammersley J M 1961 *Proc. Camb. Phil. Soc.* **57** 516
[6] Fisher M E 1965 *J. Math. Phys.* **6** 1643 App. A, Lemma III
[7] Hille E 1948 *Functional Analysis and Semi-groups Am. Math. Soc. Colloq. Publ. No. 31* (New York: American Mathematical Society)
[8] Fisher M E 1967 *Physics* **3** 255
[9] Andreev A F 1964 *Sov. Phys.-JETP* **18** 1415
[10] Isakov S N 1984 *Commun. Math. Phys.* **95** 427
[11] Janse van Rensburg E J and Whittington S G 1989 *J. Phys. A: Math. Gen.* **22** 4939
[12] Durhuus B, Fröhlich J and Jónsson T 1983 *Nucl. Phys.* B **225** [FS9] 185
[13] Guttmann A J 1989 *Phase Transitions and Critical Phenomena* vol 13, ed C Domb and J Lebowitz (London: Academic)
[14] Parisi G and Sourlas N 1981 *Phys. Rev. Lett.* **46** 871
[15] Nienhuis B 1982 *Phys. Rev. Lett.* **49** 1062
[16] Guttmann A J and Enting I G 1988 *J. Phys. A: Math. Gen.* **21** L165
[17] Camacho C J and Fisher M E 1990 *Phys. Rev. Lett.* **65** 9
[18] Singh R R P and Fisher M E 1988 *Phys. Rev.* B **37** 1980
[19] Privman V and Rudnick J 1985 *J. Phys. A: Math. Gen.* **18** L789
[20] Fisher M E and Chen J-H 1982 *Phase Transitions (Cargese 1980)* ed M Levy, J C Le Guillou and J Zinn-Justin (New York: Plenum)
[21] Randeria M and Fisher M E 1988 *Proc. R. Soc.* A **419** 181 and references therein